Journal of Biomechanics xxx (2018) xxx–xxx

Contents lists available at ScienceDirect

Journal of Biomechanics

journal homepage: www.elsevier.com/locate/jbiomech
www.JBiomech.com

High resolution three-dimensional strain mapping of bioprosthetic heart valves using digital image correlation

Mostafa Abbasi [a], Dong Qiu [a], Yashar Behnam [a], Danny Dvir [b], Chadd Clary [a], Ali N. Azadani [a,*]

[a] University of Denver, Denver, CO, USA
[b] University of Washington, Seattle, WA, USA

ARTICLE INFO

Article history:
Accepted 10 May 2018
Available online xxxx

Keywords:
Digital image correlation
Bioprosthetic heart valve
Transcatheter aortic valve replacement
Surgical aortic valve replacement
Displacement
Strain

ABSTRACT

Transcatheter aortic valve replacement (TAVR) is a safe and effective treatment option for patients deemed at high and intermediate risk for surgical aortic valve replacement. Similar to surgical aortic valves (SAVs), transcatheter aortic valves (TAVs) undergo calcification and mechanical wear over time. However, to date, there have been limited publications on the long-term durability of TAV devices. To assess longevity and mechanical strength of TAVs in comparison to surgical bioprosthetic valves, three-dimensional deformation analysis and strain measurement of the leaflets become an inevitable part of the evaluation. The goal of this study was to measure and compare leaflet displacement and strain of two commonly used TAVs in a side-by-side comparison with a commonly used SAV using a high-resolution digital image correlation (DIC) system. 26-mm Edwards SAPIEN 3, 26-mm Medtronic CoreValve, and 25-mm Carpentier-Edwards PERIMOUNT Magna surgical bioprosthesis were examined in a custom-made valve testing apparatus. A time-varying, spatially uniform pressure was applied to the leaflets at different loading rates. GOM ARAMIS® software was used to map leaflet displacement and strain fields during loading and unloading. High displacement regions were found to be at the leaflet belly region of the three bioprosthetic valves. In addition, the frame of the surgical bioprosthesis was found to be remarkably flexible, in contrary to CoreValve and SAPIEN 3 in which the stent was nearly rigid under a similar loading condition. The experimental DIC measurements can be used to characterize the anisotropic materiel behavior of the bioprosthetic heart valve leaflets and validate heart valve computational simulations.

1. Introduction

Transcatheter aortic valve replacement (TAVR) is an alternative therapy for patients with severe aortic stenosis deemed at high- and intermediate-risk for surgical aortic valve replacement (SAVR) (Adams et al., 2014; Leon et al., 2010; Smith et al., 2011). TAVR has been widely used worldwide since 2002, and to date more than 200,000 patients have undergone this minimally invasive and life-saving procedure (Seidler et al., 2017). TAVR has the potential to change the paradigm from SAVR to TAVR in low-risk younger patients with aortic valve stenosis. However, there are currently limited clinical data available regarding the long-term durability of the commercially available transcatheter aortic valves (TAVs) (Dvir et al., 2016). Furthermore, unlike surgical bioprostheses, the primary failure mechanism of TAV is not known and should therefore be investigated. In surgical bioprosthetic heart valves, leaflets degenerate through two distinct but potentially synergistic mechanisms: (i) calcification and (ii) fatigue-induced structural deterioration (Schoen et al., 1985; Schoen, 2012). It has been demonstrated that high stress regions in stented surgical bioprostheses correlate with regions of mechanical deterioration and calcification (Ferrans et al., 1978; Sacks and Schoen, 2002). Since the commercially available TAV leaflets are made from chemically treated bovine or porcine pericardium tissue, it can be postulated that the structural deterioration of TAVs occurs via the two failure mechanisms.

To assess longevity of the currently available TAVs and develop the next generation of heart valve prostheses, in-depth comparison and assessment of strain and stress of the leaflets is essential. Numerous computational models have been developed to determine stress and strain distribution of the bioprosthetic heart valve leaflets under physiological loading conditions (Abbasi et al., 2016; Gunning et al., 2014; Hsu et al., 2015; Martin and Sun, 2015). In the

* Corresponding author at: The DU Cardiovascular Biomechanics Laboratory, Department of Mechanical and Materials Engineering, 2155 E. Wesley Ave, Room 439, Denver, CO 80208, USA.
E-mail address: Ali.Azadani@du.edu (A.N. Azadani).

https://doi.org/10.1016/j.jbiomech.2018.05.020
0021-9290/

computational simulations, considering robust and accurate constitutive models for the leaflets is of the utmost importance (Holzapfel and Ogden, 2009; Humphrey, 2003). As a result, experimental validation of the computational models should be an indispensable step to confirm the accuracy and reliability of the simulations (Abbasi et al., 2016). Due to the limited temporal and spatial resolution of the currently available imaging modalities in real-world in vivo clinical cases as applied to bioprosthetic heart valves, in vitro experimental testing of the bioprostheses provides a viable alternative to characterize soft tissue mechanical properties and validate the computational simulations. High-resolution optical measurements can be regarded as an appropriate non-invasive in vitro measurement technique to assess the deformation of the leaflets and determine the strain field. A suitable and accurate optical measurement technique is three-dimensional digital image correlation (DIC) technique which becomes more readily available and more widely used in experimental mechanics (Chu et al., 1985; Luyckx et al., 2014; Palanca et al., 2015; Rogge et al., 2005; Sun et al., 2005). The DIC technique is particularly suited for determination of TAV leaflet deformation due to its high temporal and spatial resolution (Heide-Jørgensen et al., 2016). The goal of this study was to perform a side-by-side comparison of leaflet displacement and strain fields of three commonly used bioprosthetic heart valves: (i) Carpentier-Edwards PERIMOUNT Magna surgical bioprosthesis, (ii) Medtronic CoreValve, and (iii) Edwards SAPIEN 3 using a high-resolution DIC system. The obtained results can be used to characterize the anisotropic material behavior of the leaflets and validate computational models of the commercially available bioprosthetic valves.

2. Materials and methods

In this study, three different bioprosthetic heart valves with comparable size were investigated (Fig. 1). The first bioprosthetic valve was a 25-mm Carpentier-Edwards (CE) PERIMOUNT Magna aortic heart valve (Edwards Lifesciences, CA, USA). The surgical bioprosthetic valve consists of bovine pericardium leaflets mounted on an Elgiloy frame. The internal diameter of the frame is 24 mm. The second bioprosthesis was a self-expanding 26-mm Medtronic CoreValve (Medtronic, Minneapolis, MN, USA), constructed from porcine pericardial leaflets mounted on a self-expanding Nitinol stent. The third bioprosthetic valve examined in this study was a 26-mm Edwards SAPIEN 3 (Edwards Lifesciences, Irvine, CA, USA). The TAV is made from bovine pericardial leaflets mounted on a balloon-expandable cobalt-chromium stent. The thicknesses of the bioprosthetic heart valve leaflets were measured using a Mitutoyo Digital caliper. The average thickness of the leaflets of the PERIMOUNT Magna, Medtronic CoreValve, and Edwards SAPIEN 3 bioprostheses was 0.56 mm, 0.43 mm, and 0.32 mm, respectively.

For DIC measurements, graphite (synthetic powder, <20 μm, Sigma-Aldrich, St. Louis, MO) was applied to the top side of the leaflets to achieve a speckled pattern (Fig. 2). Graphite was used due to its negligible effect on the mechanical properties of soft tissue as compared to ink dyes, verified by planar biaxial testing of bovine pericardial patch. To create a suitable stochastic pattern, graphite was applied multiple times to the top side of the leaflets. Subsequently, the valves were stored in normal saline solution at the room temperature prior to the DIC measurements. All the DIC measurements were conducted in an in vitro test setup comprised of an optically clear acrylic chamber, peristaltic pump, pressure transducer, and data acquisition system (Fig. 3A). The valves were mounted inside the chamber using a silicone washer on a custom-made fixture fabricated by U-Print SE Plus 3D printer (Stratasys Ltd., MN, USA). A Masterflex peristaltic pump (Cole Parmer Instrument Co., Chicago, IL, USA) was used to fill the valve housing and apply uniform pressure within the chamber. The bioprosthetic valves were submerged fully in the chamber and care was taken to make sure no air bubbles remain in the chamber.

Fig. 1. (Left) 25-mm surgical Carpentier-Edwards PERIMOUNT Magna Pericardial bioprosthetic aortic valve. (Center) 26-mm self-expanding Medtronic CoreValve. (Right) 26-mm ballooned expandable Edward SAPIEN 3 transcatheter heart valve.

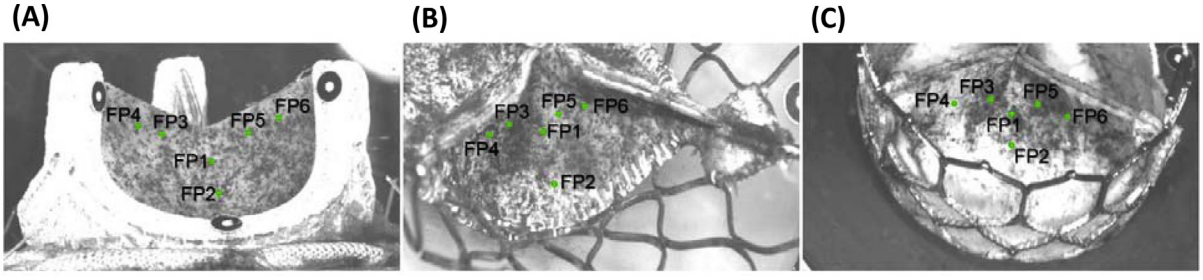

Fig. 2. Example of speckled pattern and facets points that were used for post processing of the experimental data. (A) 25-mm surgical Carpentier-Edwards PERIMOUNT, (B) 26-mm Medtronic CoreValve, and (C) 26-mm Edward SAPIEN 3.

Please cite this article in press as: Abbasi, M., et al. High resolution three-dimensional strain mapping of bioprosthetic heart valves using digital image correlation. J. Biomech. (2018), https://doi.org/10.1016/j.jbiomech.2018.05.020

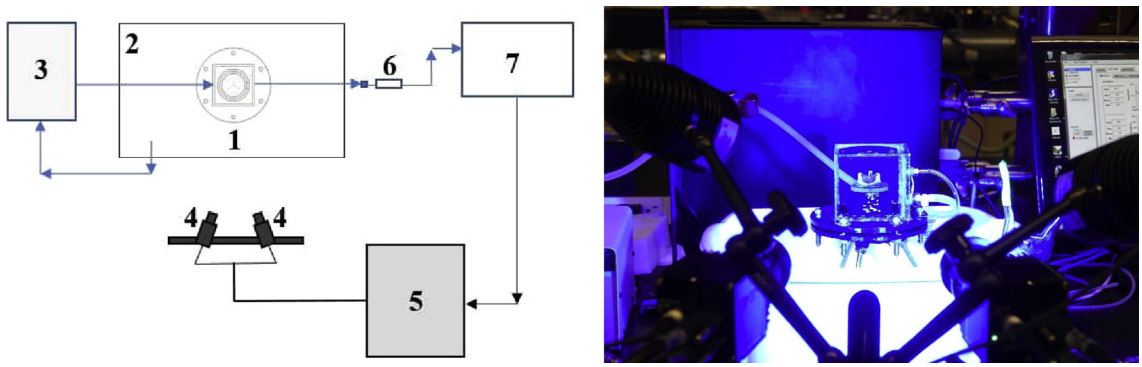

Fig. 3. (Left) A schematic overview of the in vitro DIC-based experiments consisting of (1) homemade valve housing, (2) water pool, (3) Masterflex peristaltic pump, (4) two high-speed cameras with two integrated LED light sources, (5) DIC system, (6) the pressure transducer, and (7) the data acquisition system. (Right) A photograph of the in vitro experimental setup.

Pressure in the chamber was measured continuously by a pressure transducer (Deltran, Utah Medical Products Inc., UT, USA), which was calibrated prior to the tests using a Delta-Cal Pressure Transducer (Utah Medical Products Inc., UT, USA). The chamber pressure was monitored by StatysTM software (BDC Laboratories, Wheat Ridge, CO, USA) and recorded simultaneously by a data acquisition system (NI SCC-68, National instruments, TX, USA).

DIC imaging was performed using a GOM-ARAMIS stereovision system (GOM-Optical Measuring Techniques, Braunschweig, Germany). The system consists of two high-speed cameras with a resolution of 5 megapixels (2448 × 2050 pixels) equipped with 50 mm focal length Titanar lenses (Fig. 3B). To achieve a high contrast in the speckled pattern, the valve surface was lightened by two integrated LED lights (Schneider Optische Werke, GmbH, Bad Kreuznach, Germany). The DIC system was calibrated prior to the tests to accommodate a measuring volume of 80 × 80 × 65 mm. The calibration procedure for the cameras was done based on the user manual of ARAMIS. The angle between the two cameras was ~25° and the distance between two cameras was 216 mm. Both cameras were placed at the measuring distance of 575 mm from the valve housing. For each one of the bioprostheses, DIC measurement was conducted both from top and side views in separate experiments.

A change in the pump speed resulted a corresponding change in the pressure within the testing chamber, and the chamber pressure was simultaneously monitored by StatysTM software. Prior to data collection, 10 preconditioning cycles were applied to the leaflets at a rate of 0.5 Hz. In each cycle, the pressure inside the chamber was cyclically changed from 20 mmHg to 30 mmHg. After preconditioning, the pump speed was increased from 120 rpm to 180, 300, and 480 rpm at a fixed rate of 1 Hz, corresponding to low, medium, high loading frequencies, respectively. Separate experiments were conducted for each pump setting. Loading was followed by an unloading stage and the pump speed was reduced to 120 rpm at a fixed rate of 1 Hz. Simultaneously with pressure alteration, image acquisition was triggered in the DIC system and image series were collected and stored using the ARAMIS DIC software (ARAMIS v2016, GOM, Braunschweig, Germany) at a frame rate of 10 frames per second. Following image acquisition, image processing was performed using the ARAMIS DIC software by discretizing all the images to a grid of square subsets of pixels called facet point (FP). A few sample FPs are shown in Fig. 2, e.g., FP 1 and FP 2 on the belly region and FP 3–6 parallel to the leaflet free edge. An identical facet size (19 pixels) was considered for all the three valves. Leaflet deformation was determined by tracking the movement of all the facet points. 3D surface contours of the displacement map and corresponding strain values were determined with respect to a reference configuration, i.e. chamber pressure of 30-mmHg.

3. Results

The obtained pressure curves in the in vitro test setup for the three pump settings, i.e. 180, 300, 480 rpm, are presented in

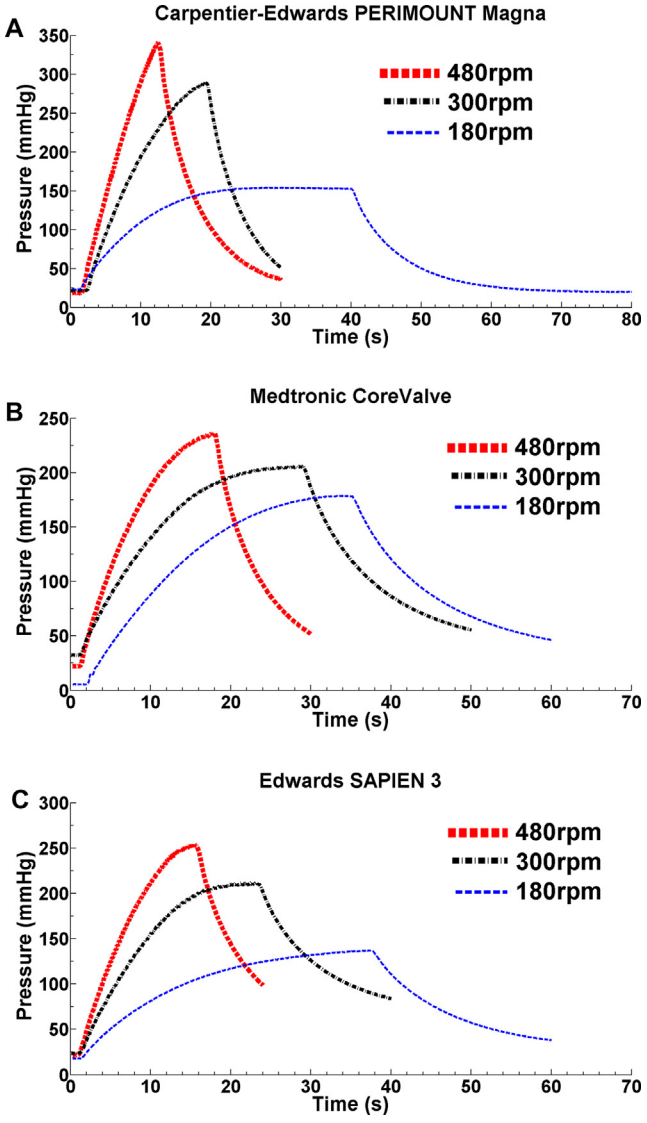

Fig. 4. Pressure curves acquired from the in vitro experimental setup during loading and unloading. (A) 25-mm surgical Carpentier-Edwards PERIMOUNT Magna, (B) 26-mm Medtronic CoreValve, and (C) 26-mm Edward SAPIEN 3.

Please cite this article in press as: Abbasi, M., et al. High resolution three-dimensional strain mapping of bioprosthetic heart valves using digital image correlation. J. Biomech. (2018), https://doi.org/10.1016/j.jbiomech.2018.05.020

Fig. 4. Three distinct pressure curves were obtained for the three pump settings, as it was expected. Pressure build-up magnitude and time were similar for the two TAV devices. However, the pressure build-up magnitude and time was higher and shorter, respectively, in the CE PERIMOUNT Magna surgical bioprosthesis compare to the two TAVs particularly in 300 and 480 rpm pump settings. For example, at pump speed of 480 rpm, the pressure build-up magnitude in the CE PERIMOUNT Magna surgical bioprosthesis was 44% and 34% higher than the Medtronic CoreValve and Edwards SAPIEN 3, respectively. At the same time, the CE PERIMOUNT Magna bioprosthesis reached to the peak pressure 30% and 19% faster than the CoreValve and SAPIEN 3, respectively. The main reason behind the difference in pressure curves between the SAV and the two TAVs was the perfectly closed leaflet geometry of the surgical bioprostheses at zero-loading condition which prohibits any central leakage upon small pressure applied to the leaflets of the surgical valve.

The representative displacement contour plots of the bioprosthetic valve leaflets at pressures of 40, 80, and 120 mmHg are presented in Fig. 5A. At 120 mmHg pressure, high displacement regions were observed at the leaflet belly region for the PERIMOUNT Magna, CoreValve, and SAPIEN 3 bioprostheses. The maximum leaflet displacement value for the PERIMOUNT Magna, Medtronic CoreValve, and Edwards SAPIEN 3 with respect to the reference configuration (chamber pressure of 30-mmHg) was 1.80, 0.80, and 0.92 mm, respectively. Unlike the CE PERIMOUNT Magna and SAPIEN 3 bioprostheses, the displacement contour for the CoreValve was not symmetric due to a subtle asymmetry in the geometry after leaflet cooptation under loading. In addition, the frame of the surgical bioprosthesis was found to be flexible under the loading conditions (Fig. 6). For instance, the maximum displacement of the frame reached to 0.63 mm at 120 mmHg pressure. However, the stent of CoreValve and SAPIEN 3 was found to be inelastic and rigid under similar loading conditions. It was

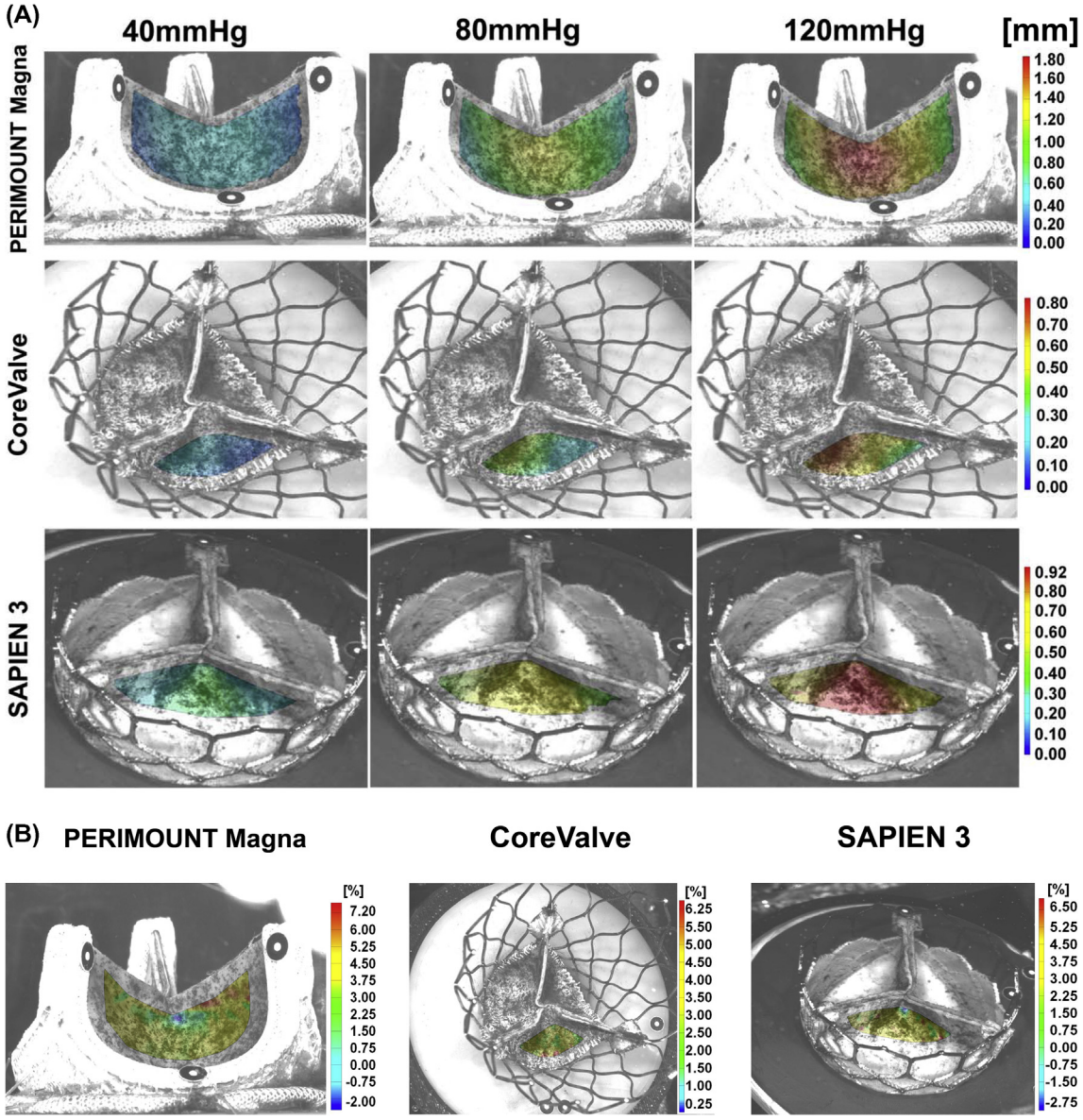

Fig. 5. (A) Displacement contour plots of the bioprosthetic valve leaflets at pressures of 40, 80, and 120 mmHg at the pump speed of 480 rpm. (B) The Green major (principal) in-plane strain contour plots of the bioprosthetic valve leaflets at pressure of 120 mmHg at the pump speed of 480 rpm. (For interpretation of the references to colour in this figure legend, the reader is referred to the web version of this article.)

Please cite this article in press as: Abbasi, M., et al. High resolution three-dimensional strain mapping of bioprosthetic heart valves using digital image correlation. J. Biomech. (2018), https://doi.org/10.1016/j.jbiomech.2018.05.020

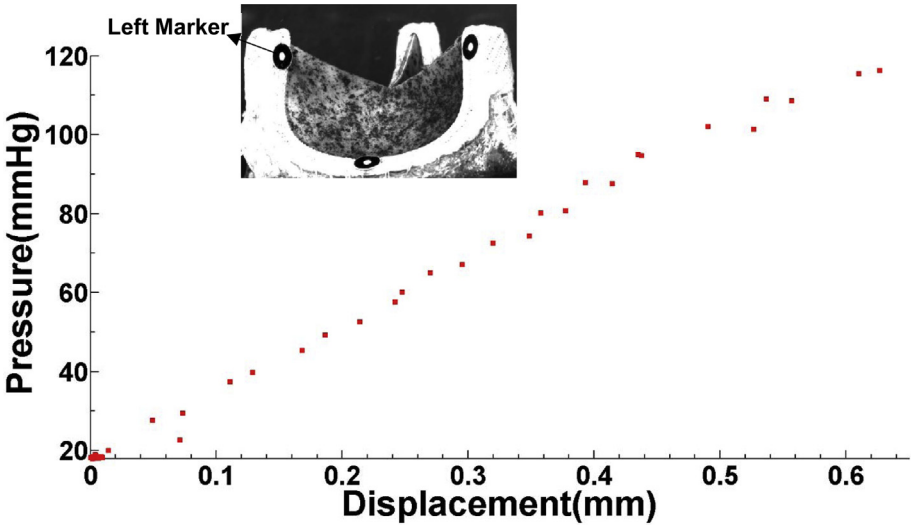

Fig. 6. Pressure–displacement curves of the left marker mounted on the PERIMOUNT Magna frame close to the commissure at the pump speed of 480 rpm.

observed that maximum displacement of the CoreValve and SAPIEN 3 stents at the commissures was 0.04 and 0.06 mm at 120 mmHg pressure, respectively. Overall, the results of the experiments show that the stent deformation of TAVs was negligible compared to the surgical bioprosthesis.

To evaluate the viscoelastic behavior of the pericardial leaflets, experimental pressure–displacement curves were obtained at the three pump speeds for the high displacement region, which was the belly region of the leaflets. Fig. 7 shows the pressure–displacement curves of FP 1, as marked in Fig. 2, on the belly region of the three bioprosthetic valves. The FP 1 coordinates with respect to the commissures at the reference pressure configuration are given in the supplementary material. It was observed that the loading and unloading curves were of different shape. Moreover, the large deformation response was not fundamentally affected by the loading rate.

Strain can be calculated and determined from the obtained displacement field. The contour maps of the major (principal) in-plane Green strain of the three bioprostheses at pressure of 120 mmHg and pump speed of 480 rpm were depicted in Fig. 5B. The contour maps were obtained from top view DIC measurements. Table 1 shows the major (principal) in-plane Green strain values in the belly region of the bioprosthetic valve leaflets in vicinity of FP1 at different pressure levels. It was observed that the maximum in-plane principal strain was increased as the chamber pressure was raised. In addition, Table 2 shows the principal Green strain values at different pressure settings for a region close to the commissures as shown by red markers in Fig. 8. For PERIMOUNT Magna and Edwards SAPIEN 3, the principal strain values were higher in the region close to the commissures than the belly region. For Medtronic CoreValve, however, the strain values were lower in the commissure region than the belly region. Nevertheless, the maximum strain value on CoreValve leaflets were found below the commissure region close to the fixed boundary edge, as marked by a blue marker in Fig. 8. The principal strain values for the region below the commissure and close to the fixed boundary edge were 1.5%, 2.3%, 3.1%, 4.6%, and 5.3%, at a pressure of 40, 60, 80, 100, and 120 mmHg, respectively.

4. Discussion

In this study, we presented an experimental framework to determine leaflet displacement field of CE PERIMOUNT Magna surgical bioprosthesis, Medtronic CoreValve, and Edwards SAPIEN 3 using 3D DIC measurements. A time-dependent uniform pressure was applied to the leaflets of the bioprosthetic valves mounted in a custom-made testing system. Through the in vitro experiments, we found that in all the three bioprosthetic heart valves the maximum leaflet displacement was generally in the upper part of the belly region. However, higher displacement values were observed in the CE PERIMOUNT Magna than CoreValve and SAPIEN 3 bioprostheses. In addition, the frame of the surgical bioprosthesis was found to be markedly flexible under the loading conditions. However, the stent of CoreValve and SAPIEN 3 was found to be rigid under the same loading condition. Frame flexibility and higher leaflet displacement magnitude of the SAV as compared to those for the two TAVs can potentially alter leaflet stress distribution and may be related to the altered long-term durability among different bioprostheses. The acquired experimental data can be used to characterize the 3D anisotropic mechanical properties of the leaflets and validate computational models of the commercially available bioprosthetic heart valves. Moreover, the experimental observations underline the fact that there are significant differences between geometry and deformation characteristics of TAVs and SAVs, which may lead to altered long term durability of the bioprostheses.

Long-term durability assessment of tissue heart valves is crucial to choose the right prosthetic heart valve for aortic valve replacement. Particularly, to expand TAVR into low-risk younger patients, TAV durability must match with that of surgical bioprostheses. Although there is no unified definition of structural valve degeneration, the rate of structural valve degeneration in surgical bioprostheses is known to be less than 15% at 10 years (Rodriguez-Gabella et al., 2017). Forcillo and colleagues (Forcillo et al., 2013) in a retrospective cohort study studied 2405 patients with a mean age of 71 ± 9 years old who underwent aortic valve replacement with Carpentier-Edwards surgical pericardial bioprostheses. They found that the overall freedom rate of valve reoperation for valve dysfunction averaged 96% ± 1% and 67% ± 4% at 10 and 20 years, respectively. It is also well known that the rate of reoperation for surgical valve dysfunction is strongly affected by age. As an example, Bourguignon and colleagues (Bourguignon et al., 2015) demonstrated that the freedom from reoperation rates attributable to structural valve deterioration in patients aged 60 or younger who received Carpentier-Edwards PERIMOUNT aortic valve were 88.3 % ± 2.4% and 38.1% ± 5.6% at 10 and 20 years, respectively. Besides clinical studies, an in vitro experiment was recently conducted in

Please cite this article in press as: Abbasi, M., et al. High resolution three-dimensional strain mapping of bioprosthetic heart valves using digital image correlation. J. Biomech. (2018), https://doi.org/10.1016/j.jbiomech.2018.05.020

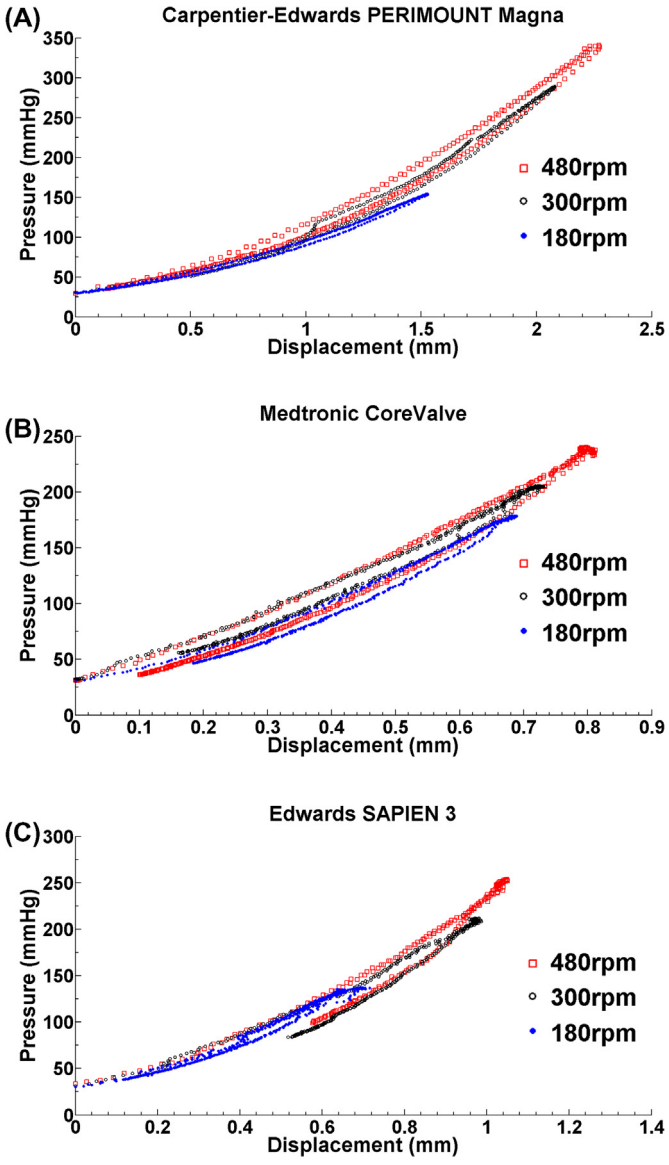

Fig. 7. Experimental pressure–displacement curves of FP 1 on the belly region of (A) 25-mm surgical Carpentier-Edwards PERIMOUNT Magna, (B) 26-mm Medtronic CoreValve, and (C) 26-mm Edward SAPIEN 3 bioprosthesis.

accordance with ISO 5840:2005 heart valve standard to assess the long-term durability of the CE PERIMOUNT Magna Ease Bioprostheses (Raghav et al., 2016). In the study, the long-term mechanical durability and hydrodynamic performance of the valve were evaluated through 1 billion cycles (equivalent to 25 years) considering mechanical wear and tear in the absence of calcification. The results showed that the Carpentier-Edwards Magna Ease valves are able withstand the mechanical environment of aortic valves for up to 25 years and perhaps even longer.

In contrary to SAVs, there is a paucity of clinical data regarding long-term durability of TAVs. Recently, Dvir and colleagues (Dvir et al., 2016) conducted a study to evaluate long-term durability of TAVs including Cribier-Edwards, Edwards SAPIEN, and Edwards SAPIEN XT for 378 patients followed for up to 10 years. Based on their results, the estimated structural valve degeneration rate was approximately 50% at 8 years. Beside the clinical observations, several finite element computational simulations have been performed to obtain stress and strain distributions of TAV leaflets (Abbasi and Azadani, 2017; Abbasi and Azadani, 2015; Abbasi et al., 2016; Hsu et al., 2015; Li and Sun, 2010; Martin and Sun, 2015; Xuan et al., 2017). The simulation results showed higher mechanical stress in TAVs compare to SAVs, affected by leaflet mechanical properties, design, and thickness. As shown in this study, the pericardial leaflet thickness employed in TAVs is less than that of surgical bioprostheses to accommodate TAVs to miniaturized catheters. A reduction in leaflet thickness increases mechanical stress on the tissue and over time can negatively influence long-term durability of the TAVs. The increased mechanical stress on TAV leaflets may explain the relatively higher rate of accelerated tissue degeneration and diminished long-term durability in TAVs. However, the simulation results must be validated by in-vivo clinical studies and by non-invasive in vitro techniques such as DIC measurements as presented in this study. In addition, it is important to note that in vitro studies, such as the one presented here, only investigate the potential modes of valve failure inherent to the design and materials used, and less towards the potential clinical modes of failure.

Biological soft tissue, including glutaraldehyde fixed bovine and porcine pericardial tissues, are viscoelastic in nature and demonstrate a number of features including hysteresis, creep, and force relaxation (Lee et al., 1984; Lee et al., 1994; Talman and Boughner, 1995). Considering the results of our experiments, the leaflets showed viscoelastic behavior as manifested by different loading and unloading paths. Histological characterization of the bovine and porcine pericardium has been carried out in the past showing that the architecture of the pericardiums are similar consisting of multiple layers of collagen bundles holding some degrees of fiber orientations (Gauvin et al., 2013). In addition, it has been demonstrated that the large deformation response of pericardial bioprosthetic materials is virtually unaffected by loading frequency (Lee et al., 1994), a phenomenon that we also observed in this study. As a result in computational modeling, the viscoelas-

Table 1
Major (principal) in-plane Green strain in the belly region of the bioprosthetic valve leaflets in vicinity of FP1 of the bioprosthetic valve leaflets at different pressures (pump speed: 480 rpm).

Pressure	40 mmHg	60 mmHg	80 mmHg	100 mmHg	120 mmHg
PERIMOUNT Magna	1.6%	2.5%	3.3%	3.6%	4.0%
CoreValve	1.6%	2.2%	3.2%	4.0%	4.6%
SAPIEN 3	1.6%	2.1%	2.7%	3.1%	3.3%

Table 2
Major (principal) in-plane Green strain at different pressure settings for a region close to the commissure shown by red markers in Fig. 8 (pump speed: 480 rpm).

Pressure	40 mmHg	60 mmHg	80 mmHg	100 mmHg	120 mmHg
PERIMOUNT Magna	2.1%	3.4%	4.3%	4.5%	5.8%
CoreValve	1.1%	1.8%	2.3%	3.0%	3.2%
SAPIEN 3	1.1%	2.4%	4.1%	4.8%	5.9%

Please cite this article in press as: Abbasi, M., et al. High resolution three-dimensional strain mapping of bioprosthetic heart valves using digital image correlation. J. Biomech. (2018), https://doi.org/10.1016/j.jbiomech.2018.05.020

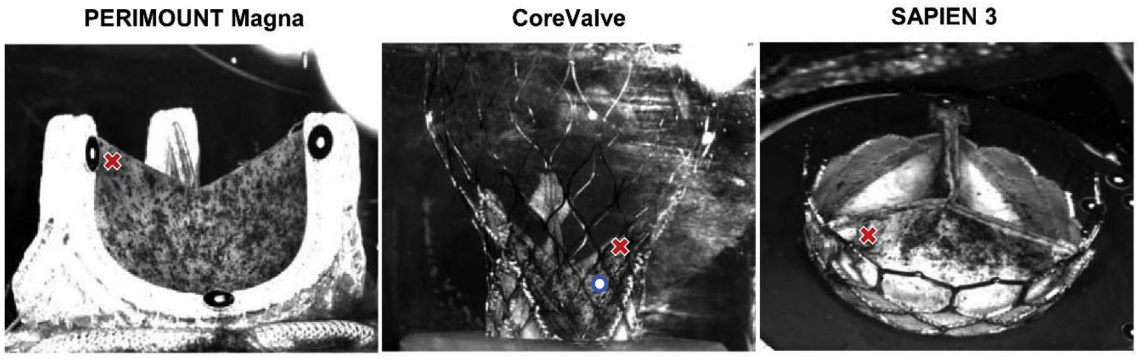

Fig. 8. Location of facet points close to the commissure region in the three bioprosthetic heart valves identified by red cross markers. The maximum strain value on CoreValve leaflets were found below the commissure region close to the fixed boundary edge as marked by a blue circle marker. (For interpretation of the references to colour in this figure legend, the reader is referred to the web version of this article.)

tic behavior of tissue heart valves is often approximated by pseudo-hyperelastic material models (Fung, 2013). Although pseudo-elastic models seem reasonable to simulate biological soft tissues, high-quality experimental data from DIC measurements are still needed to characterize the 3D anisotropic materiel models used in the computational simulations.

In summary, an in vitro DIC-based experiment was conducted to map displacement and measure strain values on three different bioprosthetic heart valves, i.e., Carpentier-Edwards PERIMOUNT Magna surgical bioprosthesis, Medtronic CoreValve, and Edwards SAPIEN 3. High displacement regions were found at the leaflet belly region of the three valves. In addition, frame of the surgical bioprosthesis was found to be noticeably flexible, in contrary to CoreValve and SAPIEN 3, in which the stent was rigid. High strain regions were found at the leaflet commissures in PREIMOUNT Magna and SAPIN 3. However, the maximum strain value on CoreValve leaflets were found below the commissure region close to the fixed boundary edge. The results of optical measurements in the DIC system can be utilized to characterize the anisotropic materiel behavior of the leaflets and validate computational simulations. The simulations would enable one to compare side-by-side different bioprosthetic heart valves and to obtain high resolution stress and strain values particularly close to the fixed boundary edge of the leaflets, a region which displacement and strain measurements are not feasible by DIC measurements. Moreover, further studies are motivated to measure leaflet deformation and strain fields under dynamic loading conditions with more number of bioprosthetic heart valves.

Conflict of interest statement

Dr. Azadani reports a financial relationship as co-founder of ReValve Medical Inc. In addition, Dr. Dvir reports consulting fees from Edwards Lifesciences, Medtronic, and St. Jude.

Acknowledgement

This work was supported by the Knoebel Center for the Study of Aging (Grant no. 142235) and partially by the American Heart Association Scientist Development Grant (AHA16SDG30920009).

Appendix A. Supplementary material

Supplementary data associated with this article can be found, in the online version, at https://doi.org/10.1016/j.jbiomech.2018.05.020.

References

Abbasi, M., Azadani, A.N., 2015. Leaflet stress and strain distributions following incomplete transcatheter aortic valve expansion. J. Biomech.

Abbasi, M., Azadani, A., 2017. Stress analysis of transcatheter aortic valve leaflets under dynamic loading: effect of reduced tissue thickness. J. Heart Valve Dis. 26, 386–396.

Abbasi, M., Barakat, M.S., Vahidkhah, K., Azadani, A.N., 2016. Characterization of three-dimensional anisotropic heart valve tissue mechanical properties using inverse finite element analysis. J. Mech. Behav. Biomed. 62, 33–34.

Adams, D.H., Popma, J.J., Reardon, M.J., Yakubov, S.J., Coselli, J.S., Deeb, G.M., Gleason, T.G., Buchbinder, M., Hermiller Jr, J., Kleiman, N.S., 2014. Transcatheter aortic-valve replacement with a self-expanding prosthesis. N. Engl. J. Med. 370, 1790–1798.

Bourguignon, T., El Khoury, R., Candolfi, P., Loardi, C., Mirza, A., Boulanger-Lothion, J., Bouquiaux-Stablo-Duncan, A.-L., Espitalier, F., Marchand, M., Aupart, M., 2015. Very long-term outcomes of the Carpentier-Edwards Perimount aortic valve in patients aged 60 or younger. Ann. Thoracic Surg. 100, 853–859.

Chu, T., Ranson, W., Sutton, M.A., 1985. Applications of digital-image-correlation techniques to experimental mechanics. Exp. Mech. 25, 232–244.

Dvir, D., Eltchaninoff, H., Ye, J., Kan, A., Durand, E., Bizios, A., Cheung, A., Aziz, M., Simonato, M., Tron, C., 2016. First look at long-term durability of transcatheter heart valves: assessment of valve function up to 10 years after implantation. Eur. J. Cardiothorac. Surg.

Ferrans, V.J., Spray, T.L., Billingham, M.E., Roberts, W.C., 1978. Structural changes in glutaraldehyde-treated porcine heterografts used as substitute cardiac valves: transmission and scanning electron microscopic observations in 12 patients. Am. J. Pathol. 41, 1159–1184.

Forcillo, J., Pellerin, M., Perrault, L.P., Cartier, R., Bouchard, D., Demers, P., Carrier, M., 2013. Carpentier-Edwards pericardial valve in the aortic position: 25-years experience. Ann. Thoracic Surg. 96, 486–493.

Fung, Y.-C., 2013. Biomechanics: mechanical properties of living tissues. Springer Science & Business Media.

Gauvin, R., Marinov, G., Mehri, Y., Klein, J., Li, B., Larouche, D., Guzman, R., Zhang, Z., Germain, L., Guidoin, R., 2013. A comparative study of bovine and porcine pericardium to highlight their potential advantages to manufacture percutaneous cardiovascular implants. J. Biomater. Appl. 28, 552–565.

Gunning, P.S., Vaughan, T.J., McNamara, L.M., 2014. Simulation of self expanding transcatheter aortic valve in a realistic aortic root: implications of deployment geometry on leaflet deformation. Ann. Biomed. Eng. 42, 1989–2001.

Heide-Jørgensen, S., Krishna, S.K., Taborsky, J., Bechsgaard, T., Zegdi, R., Johansen, P., 2016. A novel method for optical high spatiotemporal strain analysis for transcatheter aortic valves in vitro. J. Biomech. Eng. 138, 034504.

Holzapfel, G.A., Ogden, R.W., 2009. On planar biaxial tests for anisotropic nonlinearly elastic solids. A continuum mechanical framework. Math. Mech. Solids 14, 474–489.

Hsu, M.-C., Kamensky, D., Xu, F., Kiendl, J., Wang, C., Wu, M.C., Mineroff, J., Reali, A., Bazilevs, Y., Sacks, M.S., 2015. Dynamic and fluid–structure interaction simulations of bioprosthetic heart valves using parametric design with T-splines and Fung-type material models. Comput. Mech. 55, 1211–1225.

Humphrey, J.D., 2003. Continuum biomechanics of soft biological tissues. Proc. Royal Soc. a-Math. Phys. Eng. Sci. 459, 3–46.

Lee, J.M., Courtman, D.W., Boughner, D.R., 1984. The glutaraldehyde-stabilized porcine aortic valve xenograft. I. Tensile viscoelastic properties of the fresh leaflet material. J. Biomed. Mater. Res. Part A 18, 61–77.

Lee, J.M., Haberer, S.A., Pereira, C.A., Naimark, W.A., Courtman, D.W., Wilson, G.J., 1994. High strain rate testing and structural analysis of pericardial bioprosthetic materials. Biomaterials' Mechanical Properties, ASTM International.

Leon, M.B., Smith, C.R., Mack, M., Miller, D.C., Moses, J.W., Svensson, L.G., Tuzcu, E. M., Webb, J.G., Fontana, G.P., Makkar, R.R., 2010. Transcatheter aortic-valve implantation for aortic stenosis in patients who cannot undergo surgery. N. Engl. J. Med. 363, 1597–1607.

Please cite this article in press as: Abbasi, M., et al. High resolution three-dimensional strain mapping of bioprosthetic heart valves using digital image correlation. J. Biomech. (2018), https://doi.org/10.1016/j.jbiomech.2018.05.020

Li, K., Sun, W., 2010. Simulated thin pericardial bioprosthetic valve leaflet deformation under static pressure-only loading conditions: implications for percutaneous valves. Ann. Biomed. Eng. 38, 2690–2701.

Luyckx, T., Verstraete, M., De Roo, K., De Waele, W., Bellemans, J., Victor, J., 2014. Digital image correlation as a tool for three-dimensional strain analysis in human tendon tissue. J. Exp. Orthopaed. 1, 7.

Martin, C., Sun, W., 2015. Comparison of transcatheter aortic valve and surgical bioprosthetic valve durability: A fatigue simulation study. J. Biomech. Eng. 48, 3026–3034.

Palanca, M., Brugo, T.M., Cristofolini, L., 2015. Use of digital image correlation to investigate the biomechanics of the vertebra. J. Mech. Med. Biol. 15, 1540004.

Raghav, V., Okafor, I., Quach, M., Dang, L., Marquez, S., Yoganathan, A.P., 2016. Long-term durability of Carpentier-Edwards Magna Ease valve: a one billion cycle in vitro study. Ann. Thoracic Surg. 101, 1759–1765.

Rodriguez-Gabella, T., Voisine, P., Puri, R., Pibarot, P., Rodés-Cabau, J., 2017. Aortic bioprosthetic valve durability: incidence, mechanisms, predictors, and management of surgical and transcatheter valve degeneration. J. Am. Coll. Cardiol. 70, 1013–1028.

Rogge, R.D., Small, S.R., Archer, D.B., Berend, M.E., Ritter, M.A., 2013. Validation of digital image correlation techniques for strain measurement in biomechanical test models. In: Proceedings of the ASME Summer Bioengineering Conference. https://doi:10.1115/SBC2013-14540.

Sacks, M.S., Schoen, F.J., 2002. Collagen fiber disruption occurs independent of calcification in clinically explanted bioprosthetic heart valves. J. Biomed. Mater. Res. 62, 359–371.

Schoen, F.J., 2012. Mechanisms of function and disease of natural and replacement heart valves. Ann. Rev. Pathol.: Mech. Dis. 7, 161–183.

Schoen, F., Levy, R., Nelson, A., Bernhard, W., Nashef, A., Hawley, M., 1985. Onset and progression of experimental bioprosthetic heart valve calcification. Lab. Invest. 52, 523–532.

Seidler, T., Hünlich, M., Puls, M., Hasenfuß, G., Jacobshagen, C., 2017. Feasibility and outcomes of interventional treatment for vascular access site complications following transfemoral aortic valve implantation. Clin. Res. Cardiol. 106, 183–191.

Smith, C.R., Leon, M.B., Mack, M.J., Miller, D.C., Moses, J.W., Svensson, L.G., Tuzcu, E. M., Webb, J.G., Fontana, G.P., Makkar, R.R., 2011. Transcatheter versus surgical aortic-valve replacement in high-risk patients. N. Engl. J. Med. 364, 2187–2198.

Sun, W., Abad, A., Sacks, M.S., 2005. Simulated bioprosthetic heart valve deformation under quasi-static loading. J. Biomech. Eng. 127, 905–914.

Talman, E.A., Boughner, D.R., 1995. Glutaraldehyde fixation alters the internal shear properties of porcine aortic heart valve tissue. Ann. Thoracic Surg. 60, S369–S373.

Xuan, Y., Krishnan, K., Ye, J., Dvir, D., Guccione, J.M., Ge, L., Tseng, E.E., 2017. Stent and leaflet stresses in a 26-mm first-generation balloon-expandable transcatheter aortic valve. J. Thoracic Cardiovasc. Surg. 153, 1065–1073.

Please cite this article in press as: Abbasi, M., et al. High resolution three-dimensional strain mapping of bioprosthetic heart valves using digital image correlation. J. Biomech. (2018), https://doi.org/10.1016/j.jbiomech.2018.05.020